ROYAL SOCIETY
OF CHEMISTRY

PAPER

Check for updates

Exploring the potential of a potassium 4-piperidinolate/4-pyridinolate pair for reversible hydrogen storage

Alexis Munyentwali, [iD] ab Yang Yu,ab Khai Chen Tan,ab Qijun Pei,ab Zhaoji Huang,c Anan Wu [iD] *c Teng He [iD] *abd and Ping Chen [iD] abd

Hydrogen storage remains a major challenge for the widespread adoption of hydrogen as a clean and sustainable energy carrier. Chemical hydrogen storage in organic materials offers a feasible solution for safe, reversible, and high-capacity storage. However, the dehydrogenation process typically requires high temperatures due to its endothermic nature. In this study, we present a potassium 4-piperidinolate/4-pyridinolate pair (4-K-pip/4-K-pyr), which has a hydrogen storage capacity of 4.3 wt%, developed using a molecular engineering strategy that combines the effects of a heteroatom and alkali metal substitution within a single molecule to optimize dehydrogenation thermodynamics. Density functional theory (DFT) calculations indicate that this system has a favorable enthalpy change of dehydrogenation (ΔH_d) of 35.15 kJ per mol-H_2. Results from solid-state and aqueous solution experiments demonstrate the system's ability to achieve reversible hydrogen storage under moderate conditions, and most importantly, with excellent stability over multiple cycles in aqueous solution using a single catalyst. A comparison of potassium 4-piperidinolate with other hydrogen-rich compounds that have closely related structures shows that its superior hydrogen desorption performance can be attributed to its favorable ΔH_d, which arises from an effective synergy between the effects of ring nitrogen and potassium as a strong electron-donating substituent. Notably, favorable dehydrogenation thermodynamics, simple synthesis, air stability, and low material cost position the 4-K-pip/4-K-pyr system as a promising candidate for practical hydrogen storage.

1 Introduction

Hydrogen has emerged as a promising clean energy carrier for a sustainable future, thanks to its high gravimetric energy density and emissions-free conversion.[1,2] However, hydrogen's low volumetric energy density has hindered its widespread adoption due to the lack of efficient, safe, and cost-effective storage methods.[3–6] Although high-pressure compression and cryogenic liquefaction can be utilized for hydrogen storage, these traditional methods have inherent drawbacks, including high energy consumption, safety risks, high infrastructure costs, and weight losses.[7,8] To overcome these limitations, chemical hydrogen storage in condensed materials has gained considerable attention as a potential solution due to its unique

advantages, including safe and efficient high-capacity hydrogen storage achieved through controllable thermal or catalytic chemical processes. In this context, a wide array of materials, including metal hydrides,[9–11] chemical hydrides,[12,13] complex hydrides,[4,14] and liquid organic hydrogen carriers (LOHCs)[15–17] have been extensively studied for their hydrogen storage capabilities. It is essential to note that while each type of these materials has unique advantages, no existing material system fully meets all technical requirements for practical applications, particularly regarding hydrogen storage capacity, kinetics, thermodynamics, reversibility, stability, and cost-effectiveness.[18–20] Therefore, developing low-cost material systems capable of efficiently and reversibly storing hydrogen under mild conditions continues to be a significant challenge, underscoring the need for further research efforts toward innovative solutions to unlock the full potential of a hydrogen-based economy.[21,22]

Organic compounds, such as liquid organic hydrogen carriers (LOHCs), provide an effective way to reversibly store and release hydrogen through catalytic hydrogenation and dehydrogenation reactions.[23,24] Unlike other hydrogen storage materials, organic compounds have the distinct advantage of rich chemistry and structural tailorability, which can be

aDalian Institute of Chemical Physics, Chinese Academy of Sciences, Dalian 116023, China. E-mail: heteng@dicp.ac.cn

bCenter of Materials Science and Optoelectronics Engineering, University of Chinese Academy of Sciences, Beijing 100049, China

cFujian Provincial Key Laboratory of Theoretical and Computational Chemistry, College of Chemistry and Chemical Engineering, Xiamen University, Xiamen, 361005, China

dState Key Laboratory of Catalysis, Dalian Institute of Chemical Physics, Chinese Academy of Sciences, Dalian 116023, China

33614 | *J. Mater. Chem. A*, 2025, **13**, 33614–33622

This journal is © The Royal Society of Chemistry 2025

leveraged to improve hydrogen storage performance. For instance, incorporating heteroatoms, such as nitrogen (N), into cycloalkane rings has been demonstrated to improve dehydrogenation thermodynamics (ring nitrogen effect).[25] Similarly, our research group has introduced a new class of hydrogen storage materials, known as metalorganic compounds (MOCs), which are formed by substituting protic hydrogen atoms on organic molecules with lightweight alkali or alkaline earth metals such as Li, Na, and K. This strategy has been proven to improve enthalpy changes of dehydrogenation (ΔH_d) due to the strong electron-donating ability of these metals to modulate the electron densities of organic compounds (metal substitution effect).[26–29]

In the quest to develop hydrogen storage materials with dehydrogenation thermodynamics suitable for reversible hydrogen storage under moderate conditions, our research group recently proposed a new molecular engineering strategy to optimize these thermodynamics by creating an effective synergy between ring nitrogen and alkali metal substitution effects within a single molecule.[30] By studying sodium piperidinolate/pyridinolate pairs as representatives of alkali metals piperidinolate/pyridinolate systems, density functional theory (DFT) calculations and experimental findings indicated that substituting the acidic hydrogen atom of hydroxypiperidines with sodium significantly reduces ΔH_d. Interestingly, the extent of this decrease in ΔH_d is also influenced by positional isomerism. The sodium 4-piperidinolate/4-pyridinolate pair (4-Na-pip/4Na-pyr) demonstrated superior performance compared to its other positional isomers, achieving reversible H_2 storage under mild conditions. Furthermore, the type of alkali metal can also impact the hydrogen storage performance of the resulting piperidinolates. For instance, potassium compounds often display lower ΔH_d values compared to their sodium and lithium counterparts due to potassium's stronger electron-donating ability. Therefore, this study aims to explore the potential of the potassium 4-piperidinolate/4-pyridinolate pair, hereinafter referred to as 4-K-pip/4-K-pyr, as a new system for efficient reversible hydrogen storage. DFT calculations revealed that the 4-K-pip/4-K-pyr pair has a ΔH_d of 35.15 kJ per mol-H_2, which is only 62% of the ΔH_d of its parent pair (4-hydroxypiperidine/4-hydroxypyridine) and falls within the ideal range for hydrogen storage under moderate conditions.[31] H_2 absorption and desorption tests conducted in solid state and aqueous solution demonstrated that this MOC pair can achieve reversible H_2 storage at temperatures as low as 100 °C, with excellent stability over multiple cycles in aqueous solution using a bidirectional catalyst. The favorable thermodynamics, simple synthesis, air stability, and low material cost position the 4-K-pip/4-K-pyr system as a promising candidate for practical H_2 storage.

2 Results and discussion

2.1. Material design and thermodynamic calculations

In the context of optimizing the dehydrogenation thermodynamics of organic materials for hydrogen storage through structural modification, alkali metal piperidinolates display two specific structural features that have individually been shown to reduce ΔH_d, i.e., the incorporation of a nitrogen atom within the ring system[25] and the substitution of protic H by an electron-donating alkali metal at the hydroxyl group (OH) of the parent piperidinols.[26] Considering the positional isomerism in the piperidinolate and pyridinolate pairs, our previous study on sodium systems revealed that the *para* isomers exhibit superior performance in hydrogen storage.[30] Therefore, the present study focused on the *para* potassium piperidinolate/pyridinolate pair (4-K-pip/4-K-pyr) to maximize the synergistic effect of the two structural features on dehydrogenation thermodynamics. DFT calculations performed using X 1s, which is a method that combines B3LYP with neural network correction, revealed that substituting the acidic H atom in 4-hydroxypiperidine with alkali metals reduces its ΔH_d. However, the degree of ΔH_d reduction depends on the Pauling electronegativity (Z) of the alkali metal (Li, Na, and K) (Fig. 1a). Specifically, the lower the electronegativity of the alkali metal, the more pronounced the reduction in ΔH_d. For this reason, 4-K-pip has a ΔH_d of 35.15 kJ per mol-H_2 compared to 36.41 kJ per mol-H_2 and 47.42 kJ per mol-H_2 for 4-Na-pip and 4-Li-pip, respectively. This effect of substituting acidic hydrogen atoms with alkali metals on reducing ΔH_d (the alkali metal effect) is also evident when comparing potassium cyclohexanolate (K-cycloh) to its parent molecule, cyclohexanol (Fig. 1a and S1). Moreover, since the molecular structure of 4-K-pip differs from that of K-cycloh only by the incorporation of a nitrogen atom in the ring (Fig. S1), the lower ΔH_d value for 4-K-pip can reasonably be attributed to the effect of the ring nitrogen in fine-tuning the dehydrogenation thermodynamics (the heteroatom effect), which has been reported in N-heterocyclic compounds for hydrogen storage.[25,30] Therefore, these findings collectively suggest that the low ΔH_d for 4-K-pip can be ascribed to an effective synergy between the effects of the ring nitrogen and the presence of potassium as a strong electro-donating substituent in its molecular structure, as illustrated in Fig S1.

To gain a better understanding of how this structural modification strategy may affect molecular reactivity, DFT calculations also revealed that the highest occupied molecular orbital-lowest unoccupied molecular orbital (HOMO–LUMO) band gap decreases progressively from cyclohexanol to 4-H-pip and becomes significantly narrower in 4-K-pip (Fig. 1b). Similarly, the comparison of C–H bond lengths among cyclohexanol, 4-H-pip, and 4-K-pip revealed that both the incorporation of the N atom in the ring and the substitution of protic hydrogen atoms by potassium led to an elongation of C–H bonds, especially at the α positions relative to the –OK group and the N atom where the first C–H bond dissociation is very likely to occur during the dehydrogenation reaction (Fig. 1c). Interestingly, the observed trends in the HOMO–LUMO band gap and C–H bond length among cyclohexanol, 4-H-pip, and 4-K-pip are consistent with the ΔH_d values of these compounds. Therefore, comparing 4-K-pip to other hydrogen-rich molecules with closely related molecular structures strongly suggests that the dehydrogenation thermodynamics of 4-K-pip can be attributed to the synergetic effect of incorporating a nitrogen atom into the
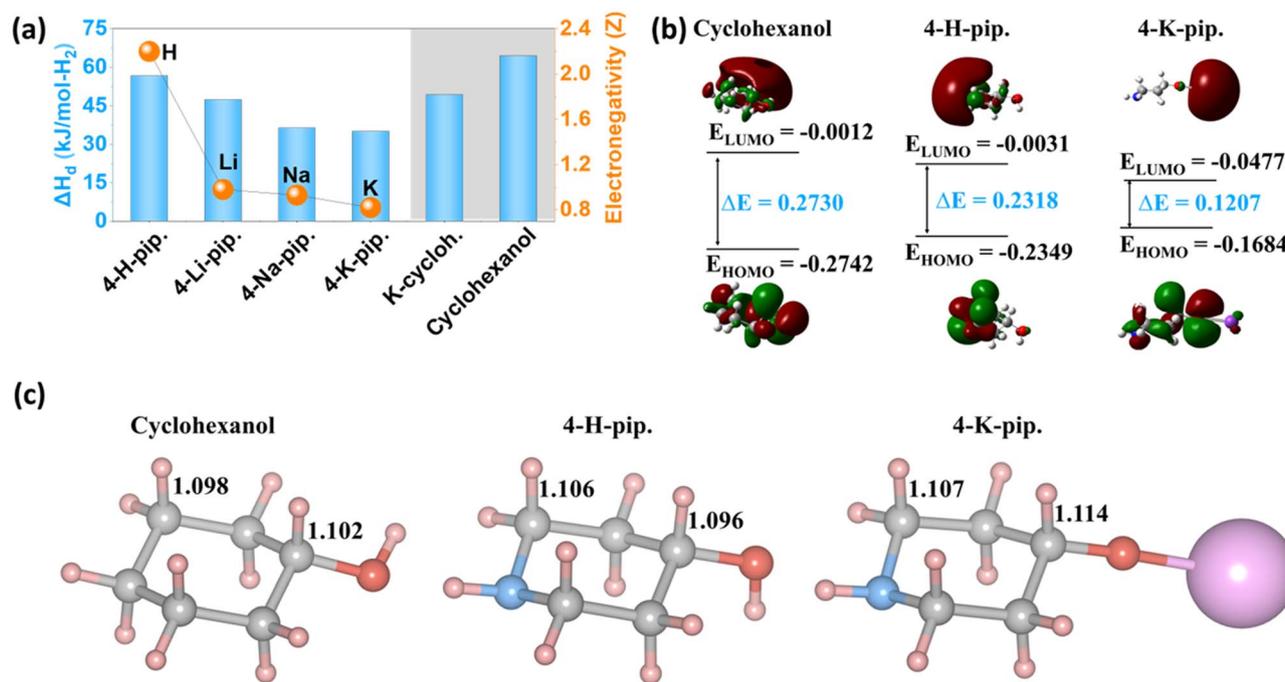
This journal is © The Royal Society of Chemistry 2025

J. Mater. Chem. A, 2025, **13**, 33614–33622 | **33615**

Fig. 1 (a) Theoretical gas-phase enthalpy changes of dehydrogenation (ΔH_d) in kJ per mol-H_2 for alkali metal 4-piperidinolates *vs.* electronegativity (Z). ΔH_d of alkali metal-4-piperidinolates are also compared to those of 4-hydroxypiperidine (4-H-pip), cyclohexanol, and potassium cyclohexanolate (K-cycloh). (b) Comparison of HOMO–LUMO band gap among cyclohexanol, 4-H-pip, and 4-K-pip. (c) Comparison of C–H bond length among cyclohexanol, 4-H-pip, and 4-K-pip.

ring structure and substituting the protic hydrogen atom with potassium, which enhances its molecular reactivity.

2.2. Material synthesis, characterization, and crystal structure analysis

Potassium 4-piperidinolate (4-K-pip) was synthesized by reacting 4-hydroxypiperidine (4-H-pip) with potassium hydride (KH) in tetrahydrofuran (THF) at 90 °C under inert conditions. Approximately one equivalent of H_2 gas was released during this reaction, indicating a complete conversion, as shown by the chemical equation in Scheme S1. A comparison of the ^1H NMR spectrum of the as-synthesized material with that of its organic substrate (4-H-pip) shows the disappearance of the –OH group proton resonance (Fig. 2a), signifying a successful deprotonation by potassium hydride. Moreover, some proton resonances shifted slightly upfield, suggesting a shielding effect likely resulting from the electron density increased by the strong electron-donating K substituent. The ^{13}C NMR spectrum of 4-K-pip (Fig. 2b) also reflects the impact of substituting the protic hydrogen with potassium, as evidenced by the downfield shifts in the resonances of some carbon atoms. 4-K-pip was also analyzed using powder X-ray diffraction (PXRD), as illustrated in Fig. 2c. The diffraction pattern of this potassium-doped material is distinctly different from that of the parent substrate, indicating the formation of a new phase. Additionally, K-cycloh and 4-Na-pip were synthesized using a similar method to compare them with 4-K-pip, in order to experimentally evaluate the effect of ring nitrogen and alkali metal

substitution on H_2 desorption kinetics and thermodynamics. The synthesis of these additional H-rich compounds from their organic substrates was confirmed by ^1H NMR spectroscopy (Fig. S2) and PXRD (Fig. S3).

On the other hand, the hydrogen-lean compound (potassium 4-pyridinolate: 4-K-pyr) was synthesized by ball milling 4-hydroxypyridine (4-H-pyr) with potassium hydride, also under inert conditions. Heating the reaction mixture at 120 °C released approximately one equivalent of H_2 gas, indicating a complete conversion, as shown by the chemical equation in Scheme S1. Alternatively, 4-K-pyr could be synthesized through a simple and cost-effective method involving the reaction of 4-H-pyr with potassium hydroxide (KOH) in an aqueous solution at room temperature. The ^1H NMR characterization of the 4-K-pyr samples synthesized using these two methods produced identical spectra, characterized by the disappearance of the NH proton resonance in 4-H-pyr (Fig. 2d), indicating a successful deprotonation. It is worth mentioning that 4-hydroxypyridine exists in equilibrium with 4-pyridone due to keto–enol tautomerism. The keto form is the most stable tautomer both in solution and in the solid state.[32,33] Moreover, unlike the slight upfield shift observed in the ^1H NMR spectrum of 4-K-pip (Fig. 2a), the resonances of all protons in the 4-K-pyr spectrum (Fig. 2d) starkly shifted upfield compared to their counterparts in the spectrum of the substrate material (4-H-pyr). This discrepancy could be attributed to the fact that electrons transferred from potassium to the aromatic ring of 4-K-pyr can be easily delocalized through strong p–π conjugation, contrary
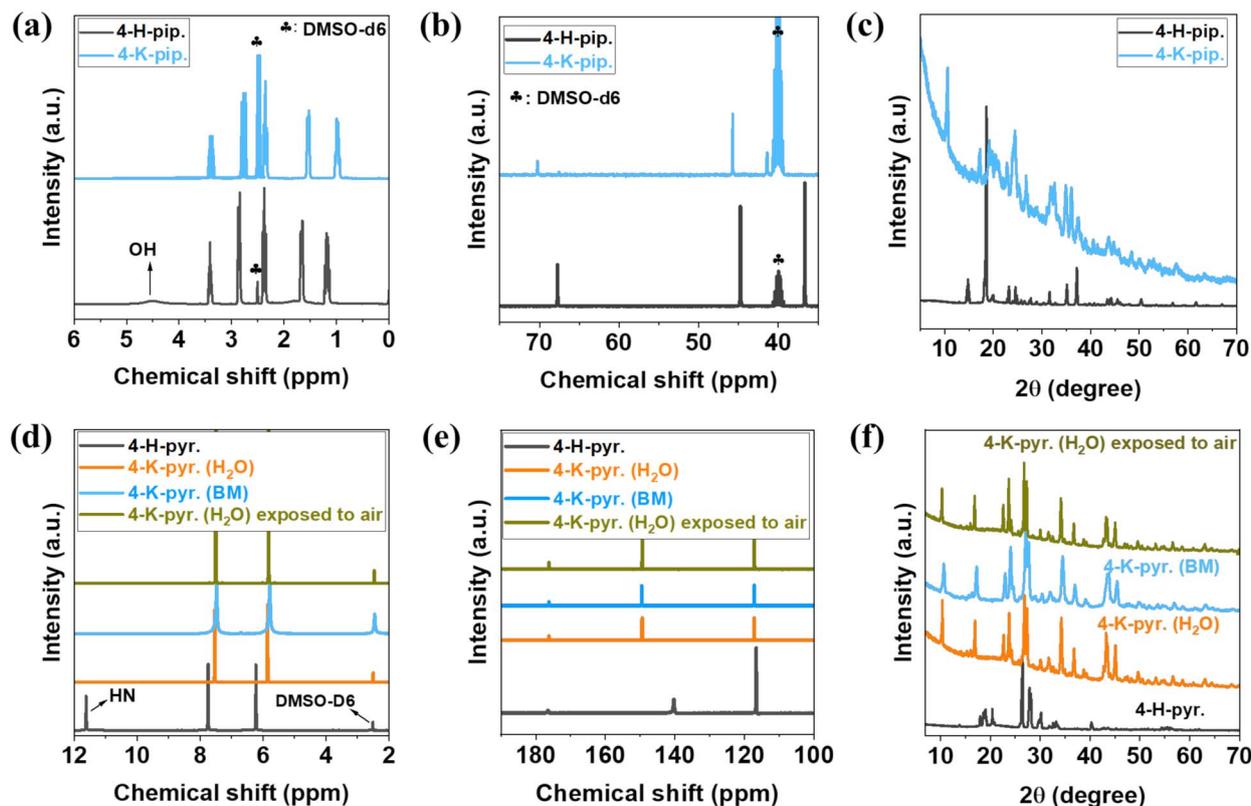
33616 | J. Mater. Chem. A, 2025, 13, 33614–33622

This journal is © The Royal Society of Chemistry 2025

Fig. 2 (a) ^{1}H NMR spectra of 4-K-pip and 4-H-pip. (b) ^{13}C NMR spectra of 4-K-pip and 4-H-pip. (c) PXRD patterns of 4-K-pip and 4-H-pip. (d) ^{1}H NMR spectrum of 4-H-pyr compared to those of 4-K-pyr samples synthesized using the ball milling method (BM) and through the reaction of 4-H-pyr with KOH in an aqueous solution (H$_2$O). (e) ^{13}C NMR spectra of 4-H-pyr compared to those of 4-K-pyr samples synthesized using the ball milling method (BM) and through the reaction of 4-H-pyr with KOH in an aqueous solution (H$_2$O). (f) PXRD patterns of 4-H-pyr compared to those of 4-K-pyr samples synthesized using the ball milling method (BM) and through the reaction of 4-H-pyr with KOH in an aqueous solution (H$_2$O).

to those of 4-K-pip, whose delocalization stems from a weaker hyperconjugation effect.

Furthermore, the 4-K-pyr samples synthesized using these two methods also have identical ^{13}C NMR spectra (Fig. 2e) and XRD patterns (Fig. 2f), confirming the effectiveness of synthesizing 4-K-pyr using inexpensive and readily available chemicals through a straightforward method under ambient conditions. Interestingly, a comparison of a fresh sample of 4-K-pyr and a sample exposed to humid air for three months revealed that this material has excellent air and moisture stability (Fig. 2d–f). It is important to note that although the H-rich compound (4-K-pip) could not be synthesized using this simple method, a high-purity sample prepared via the KH route displays high stability in dry air, as shown in Fig. S4. Therefore, both the H-lean and H-rich forms of the 4-K-pip/4-K-pyr pair are air-stable, which is a significant advantage over many other potential hydrogen storage materials currently under development for real-world applications.[34,35]

To gain further structural insights into these materials, efforts were made to solve the crystal structures of both 4-K-pip and 4-K-pyr. However, only the structure of 4-K-pyr was successfully solved thanks to its better crystallinity. The crystal structure of 4-K-pyr was solved using direct space methods combined with the first-principles molecular dynamics simulated annealing with the optimized C$_5$H$_4$NO$^-$ configuration based on lab PXRD data. Fig. S5 illustrates the Rietveld fit to the XRD pattern. Details about structural determination and Rietveld refinement can be found in the SI. The refined lattice parameters of 4-K-pyr (KOC$_5$H$_4$N) in space group Pnma (no. 62) are $a = 12.467(1)$ Å, $b = 4.1505(2)$ Å, $c = 11.4552(8)$ Å, and $V = 592.74(9)$ Å, with more crystallographic details available in the CIF (CCDC 2450241) deposited in the Cambridge Structural Database.

In the structure of 4-K-pyr (Fig. 3a), each K$^+$ connects to five C$_5$H$_4$NO$^-$ units through three K–O bonds and two K–N bonds, resulting in a square pyramidal coordination geometry (Fig. 3b) with a K–N bond length of 2.856 Å and K–O bond lengths ranging from 2.657 Å to 2.800 Å. As illustrated in Fig. 3c, the K cations are linked by O and N atoms to form K–O double zigzag chains along the b direction. These zigzag chains function as joints to interweave the 4-C$_5$H$_4$NO$^-$ anions, which are connected by K$^+$ cations head-to-toe through O and N via ionic bonding due to the specific para locations of the binding sites in the bidentate 4-C$_5$H$_4$NO$^-$.

As a result, this bonding scheme and structural architecture create a stable 3D ionic network in which the planar aromatic
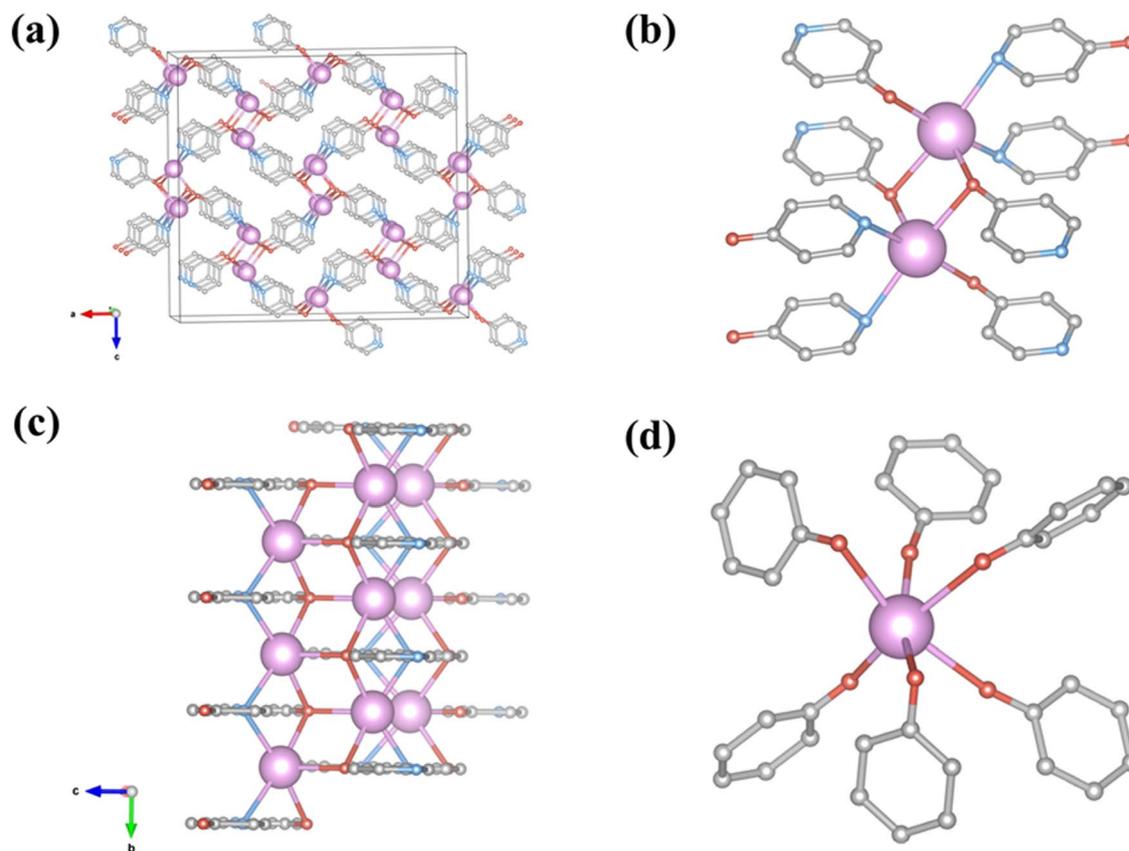
Fig. 3 (a) (011) view of the crystal structure of 4-K-pyr. Pink balls: K, red balls: O, grey balls: C, blue balls: N. H atoms are also omitted for clarity. (b) Local atom coordination in the 4-K-pyr crystal structure. H atoms are omitted for clarity. (c) (111) view of the 4-K-pyr crystal structure. (d) Local atom coordination in the crystal structure of potassium phenoxide.[36]

rings function as walls, while the K–O double zigzag chains serve as central pivot pillars (Fig. 3a). Furthermore, since the stability of a hydrogen-lean molecule also determines the thermodynamics of dehydrogenation, the crystal structure of 4-K-pyr was compared to that of potassium phenoxide (Fig S6)[36] to further elucidate the difference in ΔH_d observed between 4-K-pip and K-cycloh (Fig. 1a). As illustrated in Fig. 3d, in the structure of potassium phenoxide (K-phen), each $C_6H_5O^-$ unit binds to K^+ solely through a K–O bond. Conversely, the ditopic $C_5H_4NO^-$ ligand in the 4-K-pyr structure connects two electron-donating K^+ cations *via* K–O and K–N bonding (Fig. 3a and b), thereby stabilizing $C_5H_4NO^-$ through enhanced electron delocalization and aromaticity. This increased stability of 4-K-pyr compared to K-phen can reasonably explain why the ΔH_d of 4-K-pip is lower than that of K-cycloh (Fig. 1a).

2.3. Hydrogen absorption and desorption in the solid state

To evaluate the hydrogen storage performance of the 4-K-pip/4-K-pyr pair through chemisorption, catalytic hydrogenation and dehydrogenation reactions were initially studied in a solid state to eliminate any solvent effects. Fig. 4a illustrates the hydrogen desorption profiles of 4-K-pip catalyzed by various metal-supported catalysts from room temperature to 120 °C. The 5% Rh/C catalyst demonstrated the highest activity, enabling 4-K-

pip to release 4.1 wt% H_2 from its theoretical H_2 storage capacity of 4.3 wt% after 18 h. During this experiment, the released H_2 reached 3.6 wt% only after 3 h, suggesting fast initial kinetics. Notably, the ^{1}H NMR characterization of the post-H_2 desorption sample confirmed the dehydrogenation of 4-K-pip to 4-K-pyr with a conversion of 98.8%, which is consistent with the amount of the released H_2 measured using a volumetric method and, most importantly, without any side product. (Fig. S7). Interestingly, the H_2 desorption of 4-K-pip catalyzed by 5% Rh/C conducted from room temperature to 100 °C revealed that this material could still release 83.5% of its theoretical H_2 storage capacity after 18 h (Fig. 4b and S8). Encouraged by these experimental findings that fully support the DFT calculations suggesting favorable thermodynamics for the 4-K-pip dehydrogenation (Fig. 1a), temperature-programmed desorption coupled with mass spectroscopy (TPD-MS) of 4-K-pip mixed with the Rh/C catalyst was conducted from room temperature to 200 °C, primarily to gain deeper insights into the H_2 release temperature profile. The results revealed that 4-K-pip begins releasing H_2 at temperatures as low as 53 °C, with this release peaking at approximately 102 °C, and no other gases were released (inset of Fig. 4 b).

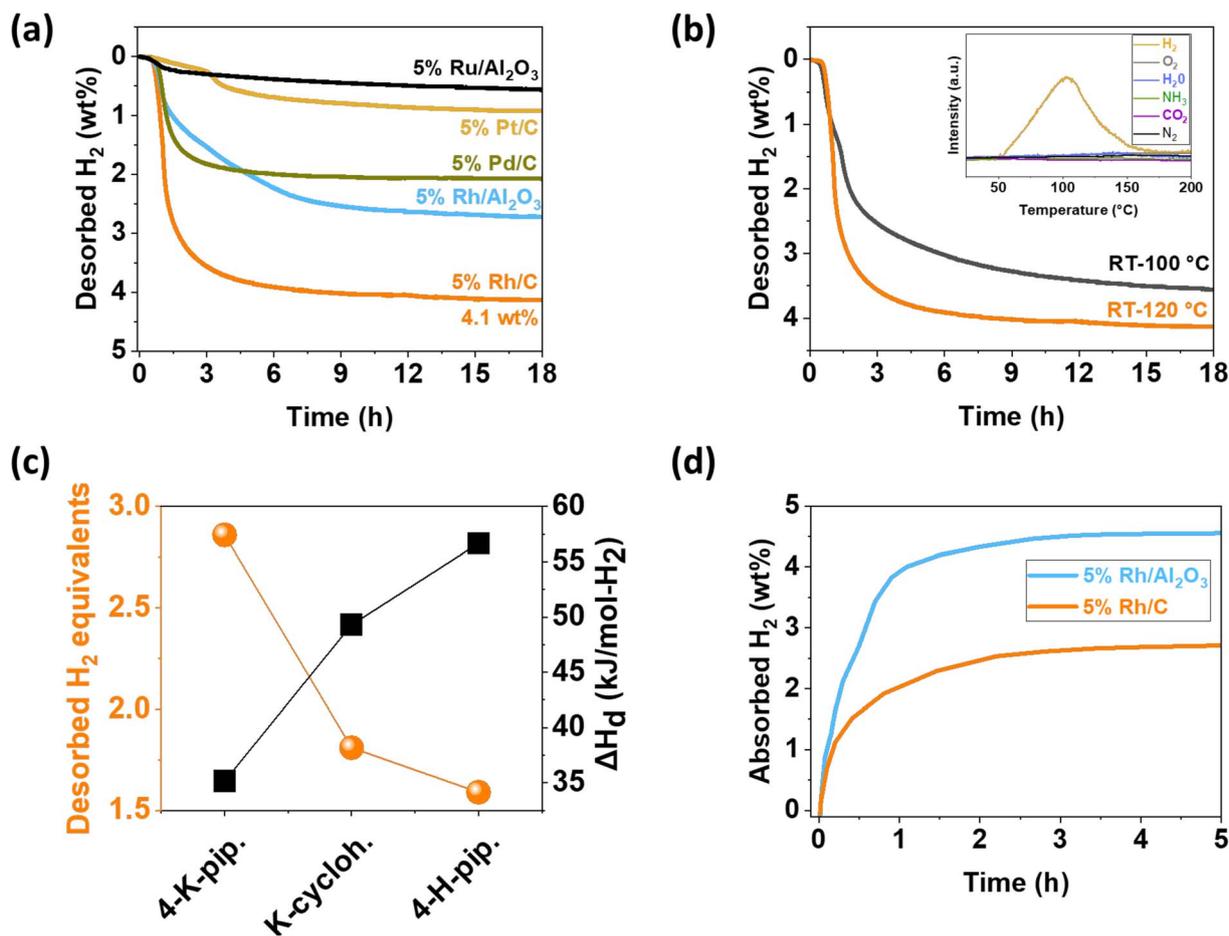Additionally, 4-K-pip was compared to its parent compound (4-H-pip) and K-cycloh, as reference materials with closely

33618 | J. Mater. Chem. A, 2025, 13, 33614–33622

This journal is © The Royal Society of Chemistry 2025

Fig. 4 (a) H_2 desorption of 4-K-pip catalyzed by different catalysts from room temperature to 120 °C. (b) H_2 desorption of 4-K-pip catalyzed by 5% Rh/C from room temperature to 100 °C compared to the same process run from room temperature to 120 °C. Inset: TPD-MS of 4-K-pip with 5% Rh/C from room temperature to 200 °C. (c) A comparison of H_2 desorption performance achieved after 18 h of reaction duration vs. theoretical ΔH_d between 4-H-pip, 4-K-pip, and K-cyclohexanolate (abbreviated as K-cycloh), temperature: 25–120 °C, catalyst: 5% Rh/C. (d) Isothermal H_2 absorption of 4-K-pyr. Catalyzed by 5% Rh/C and 5% Rh/Al$_2$O$_3$ in the solid state under 60 bar H_2 pressure at 120 °C.

related molecular structures (Fig. S1), to evaluate the effect of ring nitrogen and potassium substitution on H_2 desorption performance. As illustrated in Fig. 4c and S9, 4-K-pip significantly outperformed both 4-H-pip and K-cyloh in H_2 desorption performance, tested from room temperature to 120 °C using the 5% Rh/C catalyst. Indeed, of a total capacity of $3H_2$ equivalents, 4-K-pip could release 2.9, compared to 1.8 and 1.6 for K-cycloh and 4-H-pip, respectively. The ^1H NMR characterization of post-H_2 desorption samples revealed that these H-rich compounds were transformed into their H-lean products (Fig. S10), confirming that the released H_2 gas was produced from the dehydrogenation reaction. Notably, the trend of H_2 desorption performance is consistent with the theoretical ΔH_d values (Fig. 4c), further supporting the DFT findings regarding the synergistic effect of ring nitrogen and potassium incorporation in the 4-K-pip structure, which makes its dehydrogenation thermodynamics suitable for H_2 release under moderate conditions (Fig. 1a). Similarly, 4-K-pip was also compared to 4-Na-pip to experimentally verify the correlation between the ΔH_d of alkali metal piperidinolates and the electronegativity of alkali

metals predicted by DFT calculations (Fig. 1a). Impressively, from room temperature to 120 °C, and using the same 5% Rh/C catalyst, 4-K-pip demonstrated superior performance by releasing $2.9H_2$ equivalents, compared to 2.3 for 4-Na-pip, out of the same theoretical capacity of $3H_2$ equivalents (Fig. S11). Overall, these findings from solid-state experiments suggest that the superior H_2 desorption performance of 4-K-pip could be attributed to its suitable ΔH_d, stemming from the synergistic effect of ring nitrogen and the strong electron-donating ability of potassium, as predicted by DFT calculations.

Furthermore, the reversibility of hydrogen storage for the 4-K-pip/4-K-pyr pair in the solid state was initially evaluated by testing the hydrogen absorption capability of the hydrogen-lean molecule (4-K-pyr), catalyzed by 5% Rh/C. The main objective was to determine whether this catalyst can be effective for both the hydrogenation and dehydrogenation reactions. However, 5% Rh/C could only enable 4-K-pyr to uptake 2.7 wt% H_2 at 120 °C, even under 60 bar H_2 pressure and a high substrate-to-Rh molar ratio of 2 : 1 (Fig. 4d). This low H_2 absorption capacity is consistent with the partial hydrogenation of 4-K-pyr indicated
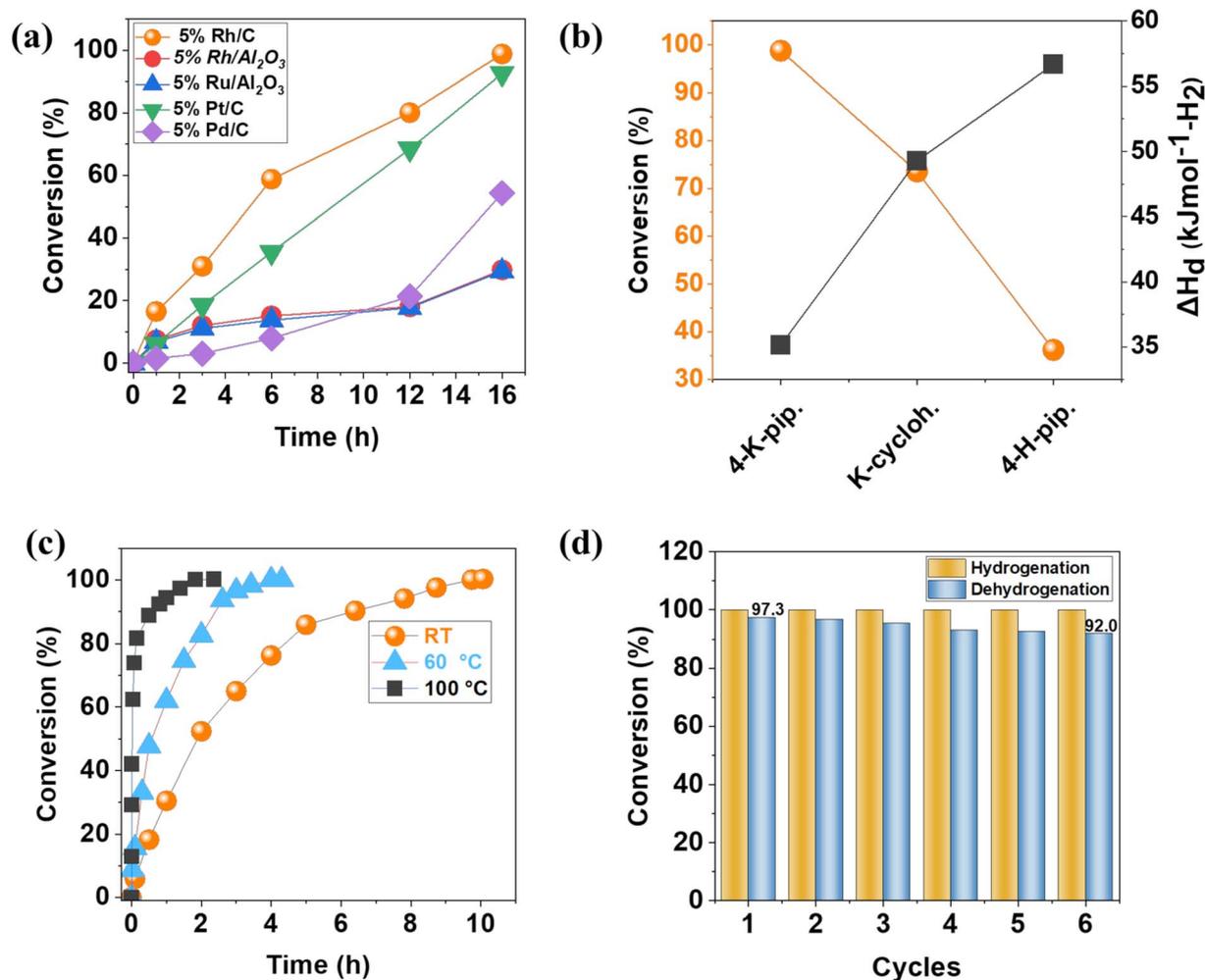
Fig. 5 (a) Dehydrogenation of 4 K-pip catalyzed by different catalysts in aqueous solution at 100 °C. (b) A comparison of substrate conversion after 16 h of reaction time *vs.* theoretical ΔH_d among 4-K-pip, 4-H-pip, and K-cycloh. (c) Hydrogenation of 4-K-pyr catalyzed by 5% Rh/C in aqueous solution at different temperatures under 40 bar H_2 pressure. (d) Hydrogenation and dehydrogenation cycles for the 4-K-pyr/4-K-pip pair in aqueous solution at 100 °C using 5% Rh/C as a bidirectional catalyst. Hydrogenation time: 3 h, dehydrogenation time: 16 h.

by ^{1}H NMR characterization of the post-H_2 absorption sample (Fig. S12). In contrast, 5% Rh/Al_2O_3, which was found to be ineffective for 4-K-pip H_2 desorption (Fig. 4b and S7), could completely hydrogenate 4-K-pyr into 4-K-pip under similar experimental conditions (Fig. 4d and S12). Unfortunately, the challenge of finding a single catalyst that is effective for both the hydrogenation and dehydrogenation of the 4-K-pip/4-K-pyr pair hindered us from conclusively assessing the cycling stability of this hydrogen storage system in the solid state.

2.4. Hydrogenation and dehydrogenation in aqueous solution

After observing that both 4-K-pip and 4-K-pyr are readily soluble in water, a green and cost-effective solvent, the reversible hydrogen storage of the 4-K-pip/4-K-pyr pair was subsequently examined in aqueous solution. This method was explored to address some challenges associated with reversible hydrogen storage in the solid state, including mass transport limitations and catalyst poisoning, which could lead to sluggish kinetics

and low conversion despite favorable thermodynamics. Notably, as shown in Fig. 5a, a catalyst screening test conducted at 100 °C with a substrate-to-metal molar ratio of 20 : 1 revealed that the dehydrogenation of 4-K-pip in aqueous solution catalyzed by 5% Rh/C could reach a conversion of 98.8% after 16 h of reaction time, with 100% selectivity to 4-K-pyr (Fig. S13). This catalyst displayed the highest activity among all other tested commercial metal-supported catalysts (Fig. 5a), as also observed during the solid-state H_2 desorption experiments (Fig. 4a). In an attempt to investigate the mechanism of this dehydrogenation reaction, *ex situ* ^{1}H NMR characterization of samples from the reaction mixture taken throughout the reaction time indicated only the presence of the initial substrate and the formed product, suggesting no detectable intermediates and no side products (Fig. S14).

To assess whether the correlation between ΔH_d and H_2 desorption performance among 4-K-pip, 4-H-pip, and K-cycloh observed in the solid-state experiments could still hold in aqueous media, a comparative analysis of the dehydrogenation

reactions of these materials was conducted using the 5% Rh/C catalyst under similar experimental conditions. Interestingly, once again, 4-K-pip not only displayed the fastest dehydrogenation rate but also reached the highest conversion (98.8%) during a 16 h-dehydrogenation process, compared to 36.2% and 73.5% for 4-H-pip and K-cyloh, respectively (Fig. 5b and S15). Additionally, as illustrated in Fig. 5b, substrate conversion percentages are also consistent with the theoretical ΔH_d values, further confirming that the superior H_2 release performance of 4-K-pip could be attributed to its favorable dehydrogenation thermodynamics, which arise from the synergistic effect of ring nitrogen and potassium presence in its molecular structure on modulating electronic properties. Based on these findings, it is essential to note that although we could not measure ΔH_d experimentally to validate our theoretical data, the consistent agreement between the theoretical ΔH_d values and the experimental H_2 desorption performance among 4-K-pip, 4-H-pip, and K-cyloh, both in solid state and in aqueous media, strongly indicates the validity of our DFT calculations.

Furthermore, the hydrogenation of 4-K-pyr in aqueous solution was also investigated, specifically employing the Rh/C catalyst. The objective was to evaluate the feasibility of reversible hydrogen storage using a single catalyst for both the hydrogenation and dehydrogenation reactions. Encouragingly, the 5% Rh/C catalyst can achieve complete hydrogenation of 4-K-pyr even at room temperature after 10 h (Fig. 5c). Raising the reaction temperature to 60 °C and 100 °C could reduce the reaction time to 4 h and 2 h, respectively. During this process, 4-K-pyr absorbed three equivalents of H_2 to produce its H-rich counterpart (4-K-pip) with 100% selectivity, as demonstrated by both ^{1}H NMR (Fig. S16) and ^{13}C NMR (Fig. S17) analyses. Driven by these promising reversibility findings, the cyclic stability of the 4-K-pip/4-K-pyr pair in aqueous solution was subsequently explored by conducting hydrogenation/dehydrogenation cycles at 100 °C. The 5% Rh/C was utilized as a bidirectional catalyst in a substrate-to-Rh molar ratio of 20 : 1. As illustrated in Fig. 5d, this pair can achieve reversible hydrogen storage with high stability over six hydrogenation/dehydrogenation cycles without a significant reduction in its storage capacity. Notably, the hydrogenation process for each cycle can reach 100% conversion in just 3 h. On the other hand, each dehydrogenation process was run for 16 h, and a slight decrease in substrate conversion was observed from 97.3% in the first cycle to 92.0% in the sixth cycle. It is important to note that while this decline in conversion could be plausibly attributed to catalyst deactivation, the 4-K-pip/4-K-pyr material system did not show any apparent structural degradation during cycling experiments (Fig. S18), indicating the excellent chemical stability for practical hydrogen storage over multiple cycles. Lastly, Table S1 compares the properties of the 4-K-pip/4-K-pyr pair, including ΔH_d, dehydrogenation temperature, air stability, hydrogen storage capacity and material cost, with some material systems commonly reported in the literature for reversible hydrogen storage. Overall, the 4-K-pip/4-K-pyr pair falls within the category of inexpensive lower-enthalpy/moderate capacity chemical hydrogen storage materials. Additionally, compared to some well-established materials such as liquid organic hydrogen carriers and metal hydrides, the 4-K-pip/4-K-pyr pair can uniquely store hydrogen reversibly under relatively mild conditions in both aqueous solution and solid state, positioning it as a promising candidate for various hydrogen storage applications.

3 Conclusion

This study demonstrates the potential of the 4-K-pip/4-K-pyr pair as a reversible hydrogen storage system in both solid state and aqueous solution. Density functional theory calculations revealed that this system has a favorable enthalpy change of dehydrogenation (ΔH_d) of 35.15 kJ per mol-H_2. Both 4-K-pyr and 4-K-pip can be synthesized by simply substituting the protic H atoms in their organic precursors with potassium. Notably, the H-lean compound of this pair (4-K-pyr) can be easily synthesized by reacting its commercial organic precursor (4-K-pyr) with KOH in aqueous solution at room temperature, and it has excellent air stability. Results from solid-state and aqueous solution experiments demonstrated the system's ability to achieve reversible H_2 storage under moderate conditions through catalytic hydrogenation and dehydrogenation reactions, along with excellent substrate conversion and product selectivity. The comparison of 4-K-pip to other hydrogen-rich compounds with closely related structures revealed that its superior hydrogen desorption performance could be attributed to its favorable ΔH_d, which stems from an effective synergy between the effects of ring nitrogen and potassium as a strong electron-donating substituent. Interestingly, a cycling stability experiment conducted at 100 °C in aqueous solution using 5% Rh/C as a bidirectional catalyst demonstrated that this system could complete six hydrogenation/dehydrogenation cycles without a significant reduction in its storage capacity, indicating great potential for reversible hydrogen storage over multiple cycles.

Author contributions

P. C. and T. H.: conceptualization, writing – review & editing, funding acquisition, supervision. A. M.: methodology, investigation, formal analysis, writing – original draft preparation. Y. Y., K. C. T., and Q. P.: formal analysis, writing – review & editing. A. W. and Z. H.: formal analysis, data curation, writing – review & editing.

Conflicts of interest

The authors declare no conflict of interest.

Data availability

Supplementary information: the data supporting this article have been included as part of the SI. See DOI: **https://doi.org/10.1039/d5ta04680g**.

This journal is © The Royal Society of Chemistry 2025

J. Mater. Chem. A, 2025, **13**, 33614–33622 | **33621**

Acknowledgements

References

1 D. Forberg, T. Schwob, M. Zaheer, M. Friedrich, N. Miyajima and R. Kempe, *Nat. Commun.*, 2016, **7**, 13201.

2 R. Zhang, H. Daglar, C. Tang, P. Li, L. Feng, H. Han, G. Wu, B. N. Limketkai, Y. Wu, S. Yang, A. X. Y. Chen, C. L. Stern, C. D. Malliakas, R. Q. Snurr and J. F. Stoddart, *Nat. Chem.*, 2024, **16**, 1982–1988.

3 U. Eberle, M. Felderhoff and F. Schüth, *Angew. Chem., Int. Ed.*, 2009, **48**, 6608–6630.

4 T. He, H. Cao and P. Chen, *Angew. Chem., Int. Ed.*, 2019, **31**, 1902757.

5 L. Schlapbach and A. Züttel, *Nature*, 2001, **414**, 353–358.

6 Y.-Q. Zou, N. von Wolff, A. Anaby, Y. Xie and D. Milstein, *Nat. Catal.*, 2019, **2**, 415–422.

7 R. K. Ahluwalia, T. Q. Hua, J. K. Peng, S. Lasher, K. McKenney, J. Sinha and M. Gardiner, *Int. J. Hydrogen Energy*, 2010, **35**, 4171–4184.

8 H. Breunig, F. Rosner, S. Saqline, D. Papadias, E. Grant, K. Brooks, T. Autrey, R. Ahluwalia, J. King and S. Hammond, *Nat. Commun.*, 2024, **15**, 9049.

9 Y. Liu, W. Zhang, X. Zhang, L. Yang, Z. Huang, F. Fang, W. Sun, M. Gao and H. Pan, *Renewable Sustainable Energy Rev.*, 2023, **184**, 113560.

10 A. Schneemann, J. L. White, S. Kang, S. Jeong, L. F. Wan, E. S. Cho, T. W. Heo, D. Prendergast, J. J. Urban, B. C. Wood, M. D. Allendorf and V. Stavila, *Chem. Rev.*, 2018, **118**, 10775–10839.

11 S. Harder, J. Spielmann, J. Intemann and H. Bandmann, *Angew. Chem., Int. Ed.*, 2011, **50**, 4156–4160.

12 C. Lang, Y. Jia and X. Yao, *Energy Storage Mater.*, 2020, **26**, 290–312.

13 J. Cashel, D. Yan, R. Han, H. Jeong, C. W. Yoon, J. A. Ambay, Y. Liu, A. T. Ung, L. Yang and Z. Huang, *Angew. Chem., Int. Ed.*, 2025, e202423661.

14 H. Wang, G. Wu, H. Cao, C. Pistidda, A.-L. Chaudhary, S. Garroni, M. Dornheim and P. Chen, *Adv. Energy Mater.*, 2017, **7**, 1602456.

15 M. J. Zhou, Y. Miao, Y. Gu and Y. Xie, *Adv. Mater.*, 2024, **36**, e2311355.

16 T. He, Q. Pei and P. Chen, *J. Energy Chem.*, 2015, **24**, 587–594.

17 A. Munyentwali, K. C. Tan and T. He, *Prog. Nat. Sci.:Mater. Int.*, 2024, **34**, 825–839.

18 M. D. Allendorf, V. Stavila, J. L. Snider, M. Witman, M. E. Bowden, K. Brooks, B. L. Tran and T. Autrey, *Nat. Chem.*, 2022, **14**, 1214–1223.

19 Q. Lai, M. Paskevicius, D. A. Sheppard, C. E. Buckley, A. W. Thornton, M. R. Hill, Q. Gu, J. Mao, Z. Huang, H. K. Liu, Z. Guo, A. Banerjee, S. Chakraborty, R. Ahuja and K.-F. Aguey-Zinsou, *ChemSusChem*, 2015, **8**, 2789–2825.

20 P. Preuster, A. Alekseev and P. Wasserscheid, *Annu. Rev. Chem. Biomol. Eng.*, 2017, **8**, 445–471.

21 P. Preuster, C. Papp and P. Wasserscheid, *Acc. Chem. Res.*, 2017, **50**, 74–85.

22 S. Sharma and S. K. Ghoshal, *Renewable Sustainable Energy Rev.*, 2015, **43**, 1151–1158.

23 P. M. Modisha, C. N. M. Ouma, R. Garidzirai, P. Wasserscheid and D. Bessarabov, *Energy Fuels*, 2019, **33**, 2778–2796.

24 D. Teichmann, W. Arlt, P. Wasserscheid and R. Freymann, *Energy Environ. Sci.*, 2011, **4**, 2767–2773.

25 E. Clot, O. Eisenstein and R. H. Crabtree, *Chem. Commun.*, 2007, 2231–2233, DOI: 10.1039/b705037b.

26 Y. Yu, T. He, A. Wu, Q. Pei, A. Karkamkar, T. Autrey and P. Chen, *Angew. Chem., Int. Ed.*, 2019, **58**, 3102–3107.

27 K. C. Tan, Y. Yu, R. Chen, T. He, Z. Jing, Q. Pei, J. Wang, Y. S. Chua, A. Wu, W. Zhou, H. Wu and P. Chen, *Energy Storage Mater.*, 2020, **26**, 198–202.

28 Z. Jing, Q. Yuan, Y. Yu, X. Kong, K. C. Tan, J. Wang, Q. Pei, X.-B. Wang, W. Zhou, H. Wu, A. Wu, T. He and P. Chen, *ACS Mater. Lett.*, 2021, **3**, 1417–1425.

29 K. C. Tan, Z. Jing, Y. Yu, Y. S. Chua, Q. Pei, D. Zheng, X. Zhang, Z. Ge, F. Zhang and T. He, *Int. J. Hydrogen Energy*, 2021, **46**, 11051–11058.

30 A. Munyentwali, Y. Yu, X. Zhou, W. Zhou, Q. Pei, K. C. Tan, A. Wu, H. Wu, T. He and P. Chen, *J. Energy Chem.*, 2025, **103**, 353–360.

31 L. Chengguang, J. Yi, Y. Xuecheng, O. Liuzhang, Z. Min and Y. Xiangdong, *Chem. Synth.*, 2022, **2**, 1.

32 M. J. Scanlan, I. H. Hillier and A. A. MacDowell, *J. Am. Chem. Soc.*, 1983, **105**, 3568–3571.

33 C. Boga, A. C. Bonamartini, L. Forlani, V. Modarelli, L. Righi, P. Sgarabotto and P. E. Todesco, *Eur. J. Org Chem.*, 2001, **2001**, 1175–1182.

34 D. Sengupta, P. Melix, S. Bose, J. Duncan, X. Wang, M. R. Mian, K. O. Kirlikovali, F. Joodaki, T. Islamoglu, T. Yildirim, R. Q. Snurr and O. K. Farha, *J. Am. Chem. Soc.*, 2023, **145**, 20492–20502.

35 J. Zhang, Y. Zhu, H. Lin, Y. Liu, Y. Zhang, S. Li, Z. Ma and L. Li, *Adv. Mater.*, 2017, **29**, 1700760.

36 R. E. Dinnebier, M. Pink, J. Sieler and P. W. Stephens, *Inorg. Chem.*, 1997, **36**, 3398–3401.

33622 | *J. Mater. Chem. A*, 2025, **13**, 33614–33622

This journal is © The Royal Society of Chemistry 2025